Preformed Oligomeric Epidermal Growth Factor Receptors Undergo an Ectodomain Structure Change during Signaling

Marisa Martin-Fernandez, David T. Clarke, Mark J. Tobin, Samantha V. Jones, and Gareth R. Jones
CLRC Daresbury Laboratory, Warrington WA4 4AD, United Kingdom

ABSTRACT Fluorescence resonance energy transfer (FRET) was used to reveal aspects of the mechanism of signal transduction by epidermal growth factor receptors (EGFR). The superpositions of epidermal growth factor (EGF), transforming growth factor-α (TGFα) and an antibody fragment (29.1) to the carbohydrate extremity of the receptor's ectodomain as measured by FRET, show that 14% of EGFRs in A431 cells are oligomerized before growth factor binding. After binding growth factor and signaling, these oligomers dissociate before releasing growth factor. Time courses of the FRET-derived distances between constitutively oligomerized EGFRs during signal transduction show a transient structural change in the extracellular domain, which occurs simultaneously with the production of intracellular Ca^{2+} signals. The FRET measurements also show a slow increase in oligomerization of EGFR monomers after growth factor binding. The structural change found in the extracellular domain of oligomeric EGFRs is similar to that shown by others for EPO, Neu, Fas, and tumor necrosis factor receptors, and may therefore be a common property of the transduction of the receptor-mediated signals.

INTRODUCTION

An epidermal growth factor receptor (EGFR) is a transmembrane receptor tyrosine kinase (RTK) that mediates the biological signal of small polypeptide mitogens, including epidermal growth factor (EGF) and transforming growth factor-α (TGFα) (Carpenter and Cohen, 1979; Derynck et al., 1984). This 170-kDa glycoprotein formed from a single polypeptide chain of 1186 amino acids can be divided into a number of functional domains (Carpenter, 1987). The heavily glycosylated 622-amino acid residue amino-terminal extracellular domain contains the growth factor binding site. A single α-helix of 23 residues forms the transmembrane region. The 542-residue cytoplasmic domain contains a 250-amino acid tyrosine kinase region and a 229-residue carboxy-terminal tail with five tyrosine residues (Hartmann and Kohlbacher, 1998), which when phosphorylated upon activation of the tyrosine kinase act as docking sites for effector proteins containing Src homology 2 (SH2) domains (reviewed by Pawson, 1995). These include Grb2, GAP, Shc, phospholipase Cγ (PLCγ), and phosphatidylinositol 3′-kinase (PI3K), which regulate Ras/Rho-like GTPases, Ca^{2+} second messenger production, and the MAP/SAP kinase pathways, leading to cell proliferation, changes in cell morphology, trafficking, and endocytosis (Carpenter, 2000).

The mechanism by which the binding of growth factor to the extracellular domain of EGFR activates the cytoplasmic tyrosine kinase is not fully understood. It is, however, known that EGFR dimerization is a requirement for activation. This is supported by data showing that EGFR cross-linking and growth factor-induced receptor dimerization lead to activation of EGFR's kinase via inter-receptor interactions (Böni-Schnetzler and Pilch, 1987; Yarden and Schlessinger, 1987a, b; Cochet et al., 1988). In light of these results, an allosteric oligomerization model for EGFR activation was developed to describe the events by which the growth factor signals are transduced by EGFR across the plasma membrane (Schlessinger, 1988). In this model inactive EGFR monomers are in equilibrium with activated EGFR oligomers, which were postulated to have higher ligand-binding affinity. Consequently, the model implies that EGF binding stabilizes the oligomeric state of EGFR in which interactions between cytoplasmic domains result in trans-autophosphorylation. It was proposed that this mechanism might be shared by other RTKs (Schlessinger, 1988).

The presence of allosteric oligomerization has been confirmed by x-ray crystallography for the fibroblast growth factor (FGF) and the insulin receptors (Plotnikov et al., 1999; Hubbard et al., 1994). Despite the absence of crystallography data, some predictions of the allosteric oligomerization model have also been verified for the EGFR using molecular biology, biochemical, and biophysical methods. High-affinity ($K_D < 1$ nM) and low-affinity ($K_D > 10$ nM) EGF/EGFR interactions were found to be a general occurrence in most cell lines, and these regulate EGFR cytoplasmic interactions with endocytic proteins (Boonstra et al., 1985; Ringerike et al., 1998). The high-affinity binding state was also found to be the means by which EGF stimulates cells both in vitro and in vivo (Aboud-Pirak et al., 1988; Defize et al., 1989; Bellot et al., 1990). Moreover, a link between high-affinity EGF binding and EGFR dimerization has been demonstrated by the increased affinity of cross-linked dimeric EGFRs (Sorokin et al., 1994) and latterly by observing the formation of dimeric high-affinity EGF/EGFR complexes using single-molecule fluorescence microscopy (Sako et al., 2000).

There is, however, evidence that EGFR activation may not just occur within an EGFR dimer, but also depend on

Submitted October 8, 2001, and accepted for publication December 21, 2001.

Address reprint requests to Gareth R. Jones, CLRC Daresbury Laboratory, Warrington WA4 4AD, United Kingdom. Tel.: 44-1925-603539; Fax: 44-1925-603124; E-mail: g.r.jones@dl.ac.uk.

0006-3495/02/05/2415/13 $2.00

interactions among EGFR dimers, secondary dimerization, heterodimerization, modulation by multiple ligands, cross-talk with other receptors, and ligand-independent lateral propagation of activation (Defize et al., 1989; Gamett et al., 1997; Verveer et al., 2000). In addition, it has also been proposed that "inactive" high-affinity EGFR may be present in significant numbers in cells without first binding EGF (Gadella and Jovin, 1995). These fluorescence resonance energy transfer (FRET) experiments in A431 cells showed high-affinity EGF/EGFR complexes to be oligomerized after growth factor challenge at 4°C. Therefore, assuming that EGF-induced dimerization, which is known to be temperature-dependent (Yarden and Schlessinger, 1987a), is totally inhibited at this temperature, Gadella and Jovin (1995) proposed that high-affinity EGFRs must have been constitutively oligomerized before binding EGF. As high-affinity receptors can be activated by EGF (Defize et al., 1989), the proposed unliganded oligomers must therefore have been prevented from phosphorylating their partner receptors' intracellular domains by the extracellular domains (Chantry, 1995). Consequently, some form of structural rearrangement in the extracellular domain of EGFR presumably would have to take place for signaling to occur after growth factor binding. This, in essence, would combine the allosteric effect proposed by Schlessinger (1988) with the concept of signal transduction occurring through constitutive dimer receptors accompanied by a ligand-induced conformational change in the EGFR's ectodomain. A mechanism such as this would be in line with results found for the EPO, Neu, Fas, and tumor necrosis factor receptors (reviewed by Jiang and Hunter, 1999).

To investigate these assertions we have measured the efficiency of FRET between fluorescently labeled monoclonal anti-EGFR Fab fragments, EGF, and TGFα bound to live A431 cells during the early stages of EGFR signal transduction. FRET is the transfer of excited-state energy from a donor fluorophore to an acceptor species with an efficiency that depends on the sixth power of donor-acceptor distances (Stryer and Haugland, 1967), and can therefore be used to quantify donor/acceptor distances in the range between 2 and 10 nm. All ligands used, EGF, TGFα, and antibody fragments to EGFR's ectodomain, bind with a 1:1 stoichiometry (Lemmon et al., 1997; Chu et al., 1997), and the antibody fragments do not oligomerize or activate EGFR (Schreiber et al., 1983). Therefore, the FRET-derived distance between these ligands can be used to investigate the state of receptor oligomerization before growth factor binding, and also to follow any conformational changes that may occur during the early events of signal transduction. Quantification of intermolecular distances via FRET was achieved by the measurement of fluorescence decay profiles (Martin-Fernandez et al., 1996, 1998). This method has the advantage of a simpler conversion of fluorescence lifetimes to donor/acceptor distance. The equivalent steady-state measurement of FRET is often ambiguous because of photobleaching and trivial transfer (Hartmann et al., 1998). The data provide evidence for the existence of constitutive high-affinity EGFR oligomers in A431 cells, and suggest that signal transduction involves a structural change in the extracellular domain of EGFR.

MATERIALS AND METHODS

Cell culture

A431 cells purchased from the European Collection of Animal Cell Cultures (ECACC) were grown in Dulbecco's modified Eagle's medium (DMEM), supplemented with 10% fetal calf serum (FCS) (v/v) and 4 mM L-glutamine (Life Technologies, Paisley, UK) at 37°C in the presence of 5% CO_2. Cells for fluorescence measurement were seeded on glass coverslips at a density of 60,000 cell/cm^2 and incubated for 24–36 h. At 12–24 h before use the cells were further incubated in DMEM containing 0.1% FCS (v/v) at 37°C in the presence of 5% CO_2. A431R cells were derived from A431 cells as described by Nelson and Fry (1997).

Protein conjugation with fluorescent dyes

Fab fragments of the monoclonal antibody 29.1 (Sigma Aldrich, Gillingham, UK) and the monoclonal antibody 255 (CalBiochem, Nottingham, UK) were prepared using the ImmunoPure Fab preparation kit 44885 (Pierce and Warrimer, Chester, UK), and characterized by molecular size exclusion chromatography on a calibrated Superose 12 FPLC column (Pharmacia, Amersham, UK). The fragments eluted as a single peak, corresponding to a molecular mass of 49,300, showing complete digestion of the antibody and removal of the Fc fragments. Fab 29.1, Fab 255, human recombinant EGF, and TGFα (Peprotech, London, UK) were dissolved in phosphate-buffered saline (PBS) to a concentration of 1 mg/ml. The pH was raised to 8.3 by adding 10% (v/v) 1 M sodium bicarbonate; 1:1 dye/protein conjugates of Alexa 488 sulfonated rhodamine-derivative were prepared as described in the Alexa labeling kit A-10235 (Molecular Probes, Leiden, The Netherlands). Erythrosin-isothiocyanate (Molecular Probes) was dissolved in DMSO to a concentration of 25 mg/ml and appropriate aliquots of dye were added to the protein for 1 h at room temperature to obtain 1:1 dye/protein conjugates. Conjugates were separated from free dye by gel filtration using a PD 10 column equilibrated with PBS and were assayed in a spectrophotometer by using molar extinction coefficients at 280 nm (protein), 488 nm (Alexa), and 529 (Erythrosin) (extinction coefficients of 71,000 and 90,000, respectively). Conjugates that deviated by $<5\%$ from a 1:1 dye/protein ratio were used. Aliquots were stored at -85°C until required.

Cell-binding experiments

Coverslips with cells at 80–90% confluency were mounted in a temperature-controlled chamber (Intracel, Herts, UK), washed for 8–10 min in Ca^{2+} and Mg^{2+}-free Hanks' balanced salt solution (Gibco, Paisley, UK), then chilled to 4°C. Cells were then incubated for 1 h at 4°C with EGF or TGFα. Growth factor was applied to the cells in a 1:2 mixture of donor-labeled growth factor to acceptor-labeled growth factor. This ensured that 80% of fluorescent receptor pairs (i.e., containing at least one donor-ligand) had a FRET partner. This was calculated using the binomial distribution. The probability of having a given number of acceptors (w) in a receptor cluster containing n receptors is $P(w) = [n!/(n - w)!w!] \times p^w q^{n-w}$. For a 1:2 donor/acceptor ratio and in the case of receptor dimers, $n = 2$, $w = 1$, p(acceptor) $= 2/3$, q donor) $= 1/3$. Substituting in the formula, $P(1) = 4/9$ and $P(0) = 1/9$. Therefore, $P(1)/P(0) + P(1) = 0.8$. A control experiment was run in which a 1:2 ratio of donor growth factor to unlabeled growth factor was used. The total growth factor concentration in each case was 150 nM, which saturates most receptor binding sites in A431 cells (Rees et al., 1984; Chu et al., 1997). For Fab 29.1 fragment-

binding experiments cells were incubated for 2 h at 4°C with a mixture of fluorescent-labeled and -unlabeled Fab fragments at a total concentration of 300 nM. A binding assay showed this concentration to saturate EGFR binding sites in A431 and A431R cells. Nonspecific binding was determined for Fab 29.1, EGF, and TGFα in the presence of 100× excess unlabeled protein and found to be <20% in all cases. For simultaneous Fab 29.1 and growth factor binding, cells were incubated for 2 h at 4°C with a 300 nM solution of acceptor-labeled Fab, and then further incubated for 1 h at 4°C with a 150 nM solution of donor-labeled growth factor. All solutions were prepared in PBS containing 0.2% (w/v) bovine serum albumin (BSA). Unbound EGF, TGFα, or Fab fragments were removed by extensively washing with ice-cold PBS. For high-affinity binding, cells were preincubated for 4 h at 4°C with a 300 nM solution of the monoclonal antibody 2E9 (TCS Biologicals, Northampton, UK) dissolved in PBS.

Intracellular calcium measurements

Cells bound to coverslips were incubated for 1 h with a 3 μM solution of internalizable Fluo-3 and 3 μM Fura-Red dye (Molecular Probes) at 37°C. Unincorporated dye was removed by washing with PBS. The cells were then cooled to 4°C and incubated for 4 h with a 300 nM solution of antibody 2E9, or for 1 h with a 300 nM solution of Fab 29.1, and then exposed to 150 nM unlabeled EGF at 4°C. Similar experiments were run with a pulse of EGF or TGFα flowing over the cells at 37°C. [Ca^{2+}] time courses were recorded on increasing the temperature to 37°C from the fluorescence intensity ratio of Fluo-3 and Fura-Red dyes (Novak and Rabinovitch, 1994). Both dyes were excited at 470 nm. A calibration was obtained using ionophore A23187-permeabilized cells in the presence of different concentrations of extracellular Ca^{2+}.

Fluorescence measurements

Fluorescence decays were recorded using time-resolved fluorescence microscopy (Martin-Fernandez et al., 1996). The field of view of the microscope was selected to be completely filled with just-confluent cells, and contained a group of ~50 cells. Samples were excited with pulsed synchrotron light at a repetition rate of 3.125 MHz on station 13.1b of the SRS at CLRC Daresbury Laboratory. Excitation of the samples was at 470 nm, and the emission was recorded between 520 and 540 nm by means of an interference filter so that the excitation light and acceptor fluorescence were eliminated. Confocal images were collected with a CW argon ion laser. Anisotropy decays were collected by measuring the components of the fluorescence decay parallel [$I_{par}(t)$] and perpendicular [$I_{per}(t)$] to the linearly polarized excitation light: $r(t) = (I_{par} - I_{per})/(I_{par} + 2I_{per})$ with a polarizing microscope as described elsewhere (Martin-Fernandez et al., 1998).

Data analysis

Fluorescence decay parameters were calculated after subtraction of the fluorescence background decay, which is composed of a 60:40 ratio of fluorescence background of the microscope and autofluorescence from cells. For the same illumination we found fluorescence background variations of <10% between cell preparations (as deduced from background values measured in 20 samples at 4°C). Time-courses of the fluorescence background were collected from unlabeled samples and subtracted from each labeled sample data set according to data frame collection time. This method resulted in the best goodness of fit (χ^2). After background subtraction, the decay data were reconvoluted with the excitation profile using the program FLUOR (Gregory et al., 1994). Fits were considered good for χ^2 between 0.8 and 1.2.

The FRET measured between different combinations of fluorescence donor and acceptor probes bound to the ectodomain of EGFR was used both to distinguish between the monomer and oligomeric states of the receptor and to detect gross structural changes; 1:1 dye-protein conjugates displayed multiexponential decay behavior in solution and were best fitted by the bi-exponential law, with a short component (for Alexa 488, $\tau = 1.12$ ns) contributing ~25% of the fluorescence decay together with a long component ($\tau = 3.75$ ns). In cells, fluorescence decays were also best fitted by the bi-exponential decay law after background subtraction. A single lifetime component of the analysis could not be attributed to an individual population of receptors. Nevertheless, the weighted mean fluorescence lifetime [$\langle\tau\rangle = (\alpha_1\tau_1^2 + \alpha_2\tau_2^2)/(\alpha_1\tau_1 + \alpha_2\tau_2)$] derived from the fluorescence decay represents the average time a fluorophore exists in the excited state, being therefore sensitive to the donor/acceptor distance and a suitable reporter for protein oligomerization (Lakowicz, 1983). The use of the weighted mean lifetime was an operational choice to avoid undue weighting of short lifetime components and light scattering. Although the value of the first-order lifetime [$(\alpha_1\tau_1 + \alpha_2\tau_2)/(\alpha_1 + \alpha_2)$] is proportional to fluorescence intensities and less biased to the contributions of long lifetime components, we chose the weighted mean lifetime for FRET calculations because it is a more stable quantity and therefore less prone to instrumental biases. Our calculations showed that the FRET-derived distances using the first- or second-order average lifetimes are in fact indistinguishable. This is because the numerical difference cancels in the calculation.

The efficiency of FRET (E) was determined from the observed fluorescence lifetimes of the donor in the presence $\langle\tau_{da}\rangle$ and absence $\langle\tau_d\rangle$ of acceptor (Lakowicz, 1983) after being corrected using $0.8\langle\tau_{da}^c\rangle + 0.2\langle\tau_d\rangle = \langle\tau_{da}\rangle$. This takes into account the 20% of donors without acceptor partner, $E = 1 - \langle\tau_{da}^c\rangle/\langle\tau_d\rangle$. Intermolecular distances were calculated by $R = R_0[E^{-1} - 1^{1/6}]$, where R_0 is the Förster radius or the distance at which the efficiency of energy transfer is 0.5, which equated to 5.7 nm. R_0 was calculated for the donor/acceptor pair from the spectral overlap integral $J(\lambda) = \int F_d(\lambda)\epsilon_a(\lambda)\lambda^4 d\lambda$, where $F_d(\lambda)$ is the normalized emission from the donor and $\epsilon_a(\lambda)$ is the normalized excitation from the acceptor multiplied by the extinction coefficient, using $R_0 = [8.8 \times 10^{23}\ \kappa^2 n^{-4} QY_d J(\lambda)]^{1/6}$ Å; QY_d is the fluorescence quantum yield of the donor in the presence of the acceptor, n is the refractive index of the medium, and κ^2 is the dipole orientation factor. We have estimated the rotational mobility of the Alexa fluorophore to be very large and have assumed a value of ⅔ for the orientation factor κ^2 in our distance calculations.

Anisotropy decays were best fitted with the bi-exponential anisotropy decay law plus a static term (Lakowicz, 1983) by $r(t) = \beta_1 \exp(-t/\phi_2) + \beta_2 \exp(-t/\phi_2) + r_\infty$, where β_i and r_∞ are the relative components of each decay and the static component, respectively. The sum of these components is equal to the anisotropy at time 0 and is related to the angles between the emission and absorption dipoles; ϕ_i are the rotational correlation times, which are a function of the rotational rates that reflect the segmental, wobbling, and global motions of the fluorescent label, ligand, and bound receptor.

RESULTS

The primary objective of this work was to use FRET to detect changes in oligomerization and structure of EGFRs during cell signaling after activation by EGF and TGFα. The duty cycle of signaling occurs over several hours, and therefore low illumination levels were necessary to avoid cell damage. Synchronization of the receptors from 50 or so cells within the field of view of the microfluorimeter was achieved by performing the growth factor challenge at 4°C. At this temperature high- and low-affinity EGF binding occurs, but endocytosis is inhibited (Gadella and Jovin, 1995; Brown and Goldstein, 1979). This method enabled us to investigate the EGF-induced oligomerization of EGFRs in the cold and provided a method of initiating synchronized cell signaling on raising the temperature to 37°C. Alternatively, synchronization was achieved by exposing cells to a

fast pulse of growth factor at 37°C through a flow system attached to the microscope's stage. To isolate the fluorescence of the high-affinity EGFRs responsible for cell signaling (Aboud-Pirak et al., 1988; Defize et al., 1989; Bellot et al., 1990), fluorescence from low-affinity EGFRs was eliminated by blocking their binding to the fluorescent growth factor (Gadella and Jovin, 1995). To further optimize the fluorescence lifetime measurements the cells were pretreated with Ca^{2+}-free buffer, which maximizes the numbers of cell surface high-affinity EGFRs (Holley et al., 1977).

The following section of the Results deals with the validation of all the above conditions using A431 cells, which overexpress EGFRs to a level of 1–2 million per cell (Fabricant et al., 1977), and A431R cells that are depleted of their high-affinity receptors (Nelson and Fry, 1997). In the remaining sections, time-resolved fluorescence data are presented that are used to compare the mechanism of signal transduction in EGFR with that of RTKs and other classes of receptors.

High- and low-affinity receptor populations in A431 cells

High- and low-affinity binding were distinguished by pretreating cells with the monoclonal anti-EGFR antibody 2E9, which specifically blocks EGF binding to low-affinity EGFRs (Defize et al., 1989). This antibody binds to the protein core of EGFR with a 1:1 stoichiometry without affecting the state of oligomerization of the receptor. The percentage of high-affinity receptors on the surface of confluent A431 cells was determined by comparing the residual fluorescence intensity of untreated cells and cells pretreated with mAb 2E9, after incubating cells with EGF labeled with Alexa 488 (Al-EGF) and washing at 4°C to remove unbound dye-growth factor conjugate. The relative affinities of Al-labeled and unlabeled growth factor were compared by titration against each other while bound to cells (Fig. 1 *A*). This showed that the fluorescent label had not changed the growth factor's affinity for its receptor.

Pretreatment of cells with mAb 2E9 reduced the fluorescence intensity from bound Al-EGF by 93% over that from untreated cells after correction for instrumental background and cell autofluorescence (see Methods), indicating that 7% of cell surface EGFRs were high-affinity (bars 1–3 in Fig. 1 *B*). This is in agreement with previous studies, which have shown that between 1 and 12% of EGFRs exhibit high-affinity EGF binding (Rees et al., 1984; Defize et al., 1989; Gadella and Jovin, 1995). The same fluorescence readings were obtained for Al-TGFα binding before and after pretreatment with mAb 2E9.

Previous work has shown that the number of cell surface high-affinity EGFRs is decreased at high cell density (Lichtner and Schirrmacher, 1990). Holley et al. (1977) showed that EGFRs were removed from the surface by sequestration as cells approached confluence, rendering them unable to bind growth factor. This was proposed as the mechanism for cell density-induced down-regulation of growth factor action, sequestered receptors being termed "cryptic." However, incubation of high-density A431 cultures in Ca^{2+}-free buffer for as little as 10 min at 37°C both increases the number of surface receptors able to bind growth factor and restores mitotic activity to high-density cultures (Holley et al., 1977; Suarez-Quian and Byers, 1993). Our work shows that Ca^{2+}-free buffer treatment of high-density A431 cultures resulted in an increase in high-affinity EGF and TGFα binding from 7% to 14% (bar 7 in Fig. 1 *B*), the latter value approximating to the 12% previously observed in low-density cultures (Rees et al., 1984). It would appear that this treatment returns cryptic EGFRs to the cell surface. Ca^{2+}-free buffer treatment was therefore used in this work before fluorescence lifetime measurements to maximize signals from high-affinity EGFRs (Fig. 1 *B*).

The modified cell line A431R is derived from A431 cells by the specific suppression of EGFR tyrosine kinase activity (Nelson and Fry, 1997). The absence of fluorescence above background from confluent A431R cells exposed to Al-EGF after blocking low-affinity EGFRs with mAb 2E9 (bar 5 in Fig. 1 *B*) is consistent with the absence of high-affinity EGF binding in these cells (Nelson and Fry, 1997). Fig. 1, *C* and *D* are typical views of A431 and A431R cells, respectively, exhibiting their characteristic morphologies, the latter appearing flattened. The treatment of confluent A431R cells with Ca^{2+}-free buffer results in the restoration of cryptic high-affinity EGFRs to a level approaching 5% of the total growth factor binding capacity (Fig. 1 *B*). These data provide additional confirmation that the inhibited growth of A431R cells due to cell-cell contact results from the down-regulation of high-affinity receptors.

The absence of high-affinity EGFRs in confluent A431R cultures should have provided a good experimental control for high-affinity EGFR activity, but the fluorescence displayed by Al-EGF/TGFα after treatment with Ca^{2+}-free buffer and the low-affinity EGFR blocker mAb did not provide enough signal above background for meaningful lifetime analysis. However, besides the morphological differences between A431 and A431R cells observed in Fig. 1, *C* and *D* attributable to differences in actin organization, the two cell types have similarly large numbers of EGFRs, indistinguishable cell cycle characteristics, and respond identically to growth factor (Nelson and Fry, 1997). Therefore, we have used Ca^{2+}-untreated A431R cells as control samples.

High-affinity EGFRs are oligomeric after binding growth factor at 4°C

The state of oligomerization of high-affinity EGFRs on A431 cells maintained at 4°C after growth factor binding was determined by comparison of the fluorescence lifetimes

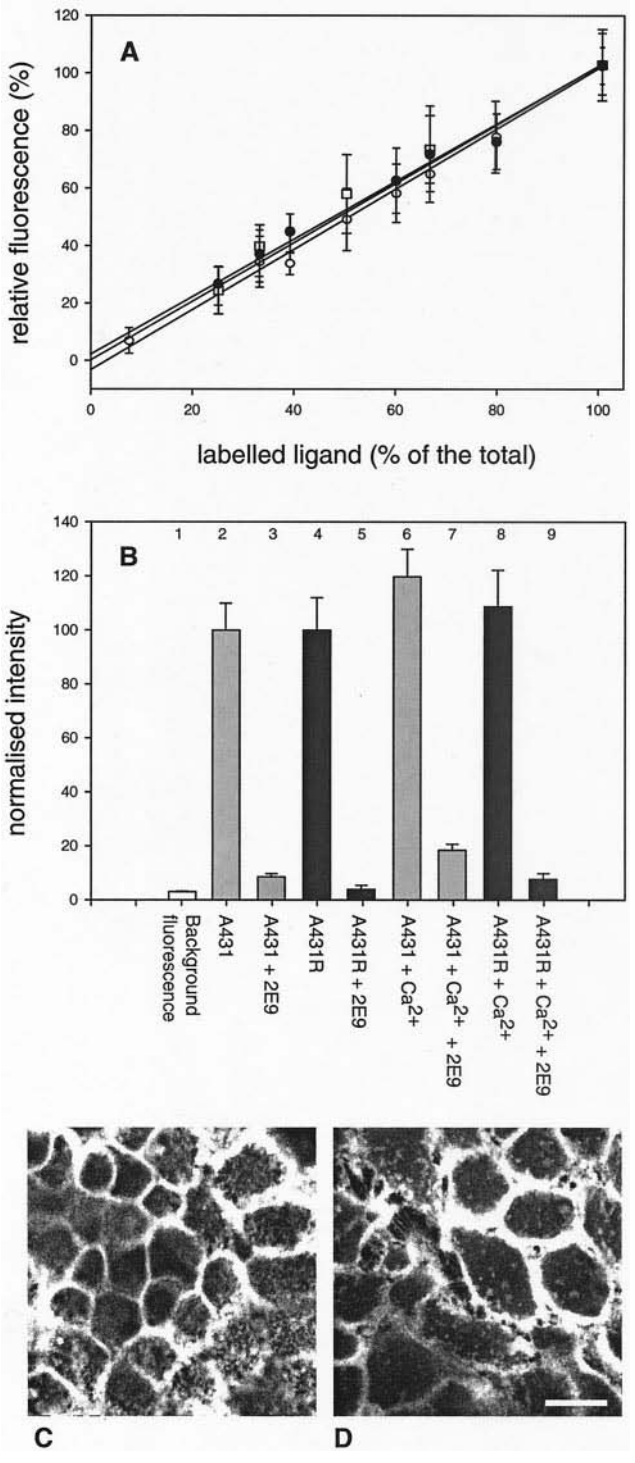

FIGURE 1 (*A*) Competitive binding of Al-EGF/unlabeled EGF (*filled circles*), Al-TGFα/unlabeled TGFα (*squares*), and Al-Fab 29.1/unlabeled Fab29.1 (*open circles*). A431 cells were incubated with 150 nM EGF or 300 nM Fab 29.1 (total concentration) at various ratios of unlabeled-ligand/Al-ligand while being maintained at 4°C to inhibit endocytosis, as described in Materials and Methods. (*B*) Histogram of the relative fluorescence intensity from A431 and A431R cells labeled with Al-EGF at 4°C. Results from cells treated with Ca^{2+}-free buffer before EGF challenge are indicated as Ca^{2+} in bar labels. For high-affinity binding, cells were pre-incubated for 4 h at 4°C with a saturating concentration (300 nM) of mAb 2E9 (+2E9 in bar labels). Results are the mean of at least three independent experiments. (*C*) Fluorescence confocal image of surface-bound Al-EGF to A431 cells. The thickness of the sections is 0.7 μm. (*D*) Fluorescence confocal image of surface-bound Al-EGF to A431R cells. Bar = 20 μm.

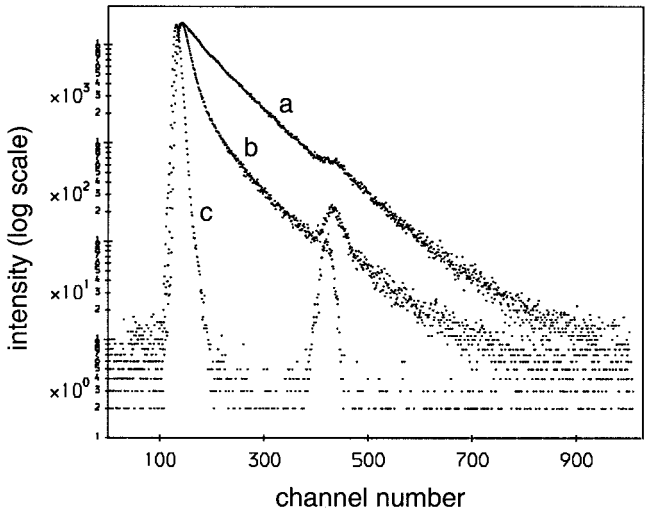

FIGURE 2 Selected donor fluorescence decays (raw data). (*a*) Fluorescence decay profile of Al-TGFα bound to A431 cells in a 1:2 ratio with unlabeled TGFα (absence of FRET); (*b*) fluorescence decay profile of donor Al-TGFα bound to A431 cells in a 1:2 ratio with acceptor Er-TGFα after pretreatment with mAb 2E9 (showing FRET); (*c*) the pulsed instrumental response function. The time calibration is 0.046 ns/channel.

of FRET donor Al-EGF or Al-TGFα, with their unlabeled and energy transfer acceptor erythrosin isothiocyanate (Er)-labeled counterpart (Fig. 2) in a 1:2 donor/acceptor ratio.

Fig. 3 *A* shows the observed weighted mean fluorescence lifetimes of donor-labeled growth factors bound to A431 and A431R cells. The fluorescence lifetime of Al-EGF bound to A431 cells in a 1:2 ratio with unlabeled EGF, and therefore in the absence of FRET, was 3.51 ns. After blocking low-affinity EGFR sites with the mAb 2E9, whose binding did not affect the fluorescence lifetime of Al-EGF, the fluorescence lifetime of donor Al-EGF bound to high-affinity EGFR with acceptor Er-EGF had decreased to 3.25 ns (bars 1 and 2 in Fig. 3 *A*). This level of quenching is small but clearly detectable above experimental noise, and therefore confirms that the high-affinity EGFR population contains a substantial proportion of oligomeric receptors after binding EGF at 4°C, as previously reported (Gadella and Jovin, 1995). The recent work of Sako et al. (2000) would suggest that the oligomeric state of the high-affinity EGFRs is in fact dimeric, although our experiment cannot distinguish between dimers and higher oligomers. A considerably smaller degree of fluorescence lifetime quenching was observed when low-affinity EGFRs were left unblocked, suggesting that there was no large shift in the population from monomers to oligomers after EGF binding

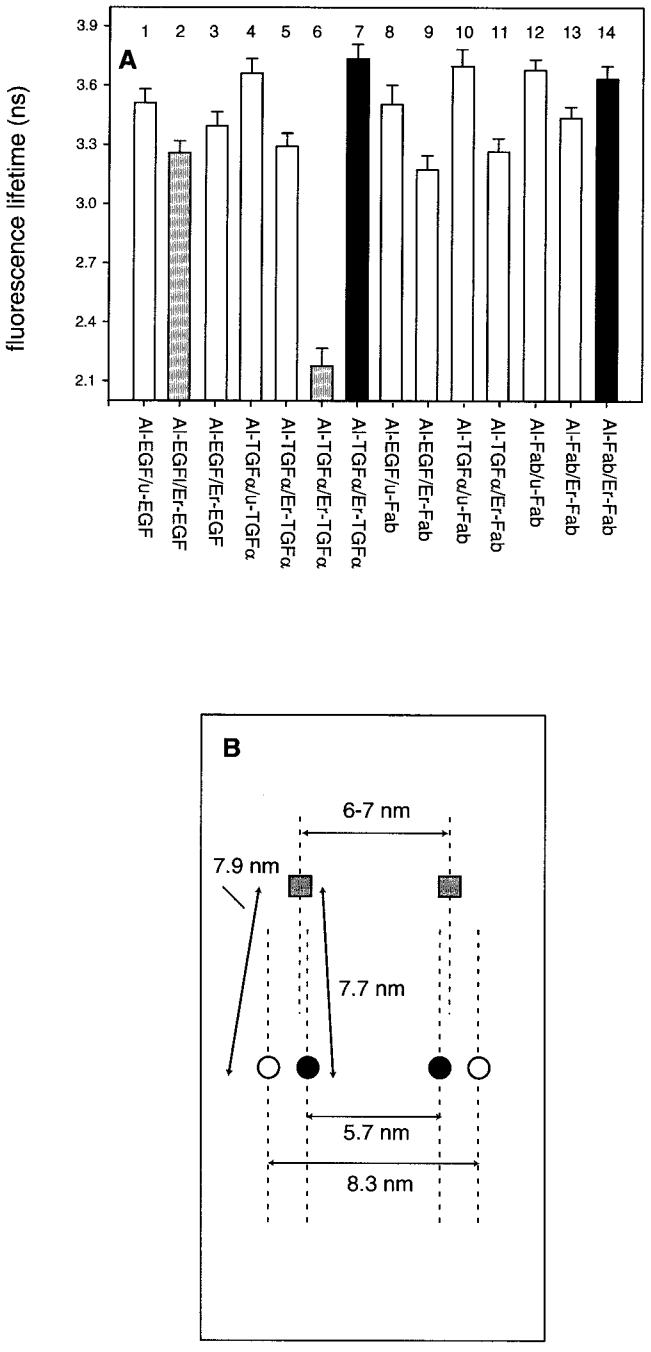

FIGURE 3 (*A*) Histogram showing the weighted mean donor lifetimes of EGF, TGFα, and Fab 29.1 fragments bound to EGFRs showing different degrees of quenching due to FRET. The open bars show results from A431 cells treated with Ca^{2+} buffer and incubated with a 1:2 mixture of donor labeled growth factor and unlabeled growth factor (Al-growth factor/u-growth factor); donor-labeled growth factor and acceptor-labeled growth factor (Al-growth factor/Er-growth factor); donor-labeled growth factor and unlabeled Fab 29.1 fragment (Al-growth factor/u-Fab); or donor-labeled growth factor and acceptor-labeled Fab 29.1 fragment (Al-growth factor/Er-Fab). Gray bars are results from A431 cells after incubation with 2E9. Black bars are results from A431R cells, which were not pre-incubated with Ca^{2+}-free buffer, as this would have resulted in returning high-affinity EGFRs to the cell surface. Binding incubations and decay measurements were performed at 4°C and results are the mean of at least three independent experiments. Error bars represent standard deviations. (*B*) Relative positions between the fluorophores conjugated to EGF (*open circles*), TGFα (*filled circles*), and Fab 29.1 (*squares*) determined from the fluorescence lifetime data in (*A*) after correction to take into account the 20% donor-donor labeled receptors (see Materials and Methods).

TABLE 1 Anisotropy decay parameters for the fluorescent ligands bound to EGFRs

	β_1	ϕ_1	β_2	ϕ_2	r_∞
Al-EGF*	0.09	0.12	0.06	4.80	0.05
Al-EGF†	0.10	0.11	0.05	4.58	0.06
Al-TGFα	0.05	0.17	0.02	5.02	0.04
Al-Fab	0.13	0.49	0.04	7.02	0.02

*Bound to high-affinity EGFR.
†Bound to high- and low-affinity EGFR. Results are the mean of three independent experiments.

at 4°C (bar 3 in Fig. 3 *A*), in agreement with previous observations (Gadella and Jovin, 1995).

The data in Fig. 3 *A* were used, after correction to take into account the 20% donor/donor emission (see Materials and Methods), to determine the efficiency of FRET and hence the apparent FRET distances between donor and acceptor species. An average distance between EGF molecules bound to high-affinity receptors of 8.3 nm was determined from the efficiency of energy transfer, using the Förster distance (R_0) for this donor/acceptor pair of 5.7 nm. This EGF-EGF distance is in agreement with that predicted by Sako et al. (2000), but longer than that estimated by Gadella and Jovin (1995) using the less accurate photobleaching FRET technique (Hartmann et al., 1998). The fluorescence anisotropies of bound donor EGF were low, most likely signifying relatively free dye rotations (Table 1) because rapid depolarization by homo-FRET ($R_0 \sim 4.6$ nm) should be very small at the FRET efficiencies measured. The anisotropy of Al-EGF bound to nontransferring low-affinity EGFRs (Table 1) gave similar values, suggesting that we can indeed discount unfavorable molecular orientations of the donor with respect to the acceptor that might degrade the accuracy of the measurement (Haas et al., 1978).

On binding the TGFα energy transfer pair to high-affinity EGFRs at 4°C, the fluorescence lifetime of donor Al-TGFα was quenched from 3.66 ns to 2.18 ns (bars 4 and 6 in Fig. 3 *A*), corresponding to a TGFα−TGFα distance of 5.7 nm. The fluorescence anisotropy for Al-TGFα was lower than for Al-EGF (Table 1), and this might be due to the presence of some homo-FRET, consistent with a TGFα−TGFα distance 2.6 nm shorter than that found for EGF. This gives a half-distance difference of 1.3 nm, which is well within the growth factors' largest molecular dimension of ~3.5 nm (Harvey et al., 1991; Kohda and Inagaki, 1992).

There are three possible explanations for the apparent intergrowth factor distance difference between EGF and TGFα. First, the locations of the dye conjugation sites on

EGF and TGFα could be different. Second, the binding orientation of EGF and TGFα on EGFRs could also be different. Third, binding sites for EGF and TGFα could be at different locations on the EGFR, as previously proposed by Winkler et al. (1989) from antibody blocking experiments. Further information on the location of growth factor binding sites was obtained by determining the distances between donor Al-EGF or Al-TGFα and acceptor (Er)-labeled Fab fragments of a monoclonal antibody (Fab 29.1) simultaneously bound to EGFR. The Fab 29.1 antibody is known to bind the carbohydrate moiety situated at the extremity of the extracellular domain at some distance from the growth factor binding site (Yarden et al., 1985). The fluorescence intensities of Al-EGF and Al-TGFα bound to untreated cells and cells saturated with unlabeled Fab 29.1 were identical, confirming that growth factor binding was not impeded by the Fab fragment. Fluorescence decay profiles of Al-EGF and Al-TGFα bound to EGFR in cells preincubated either with unlabeled Fab 29.1 or acceptor Er-Fab 29.1 showed FRET-induced donor lifetime quenching in the presence of acceptor (bars 8–11 in Fig. 3 *A*). The fluorescence lifetime of Al-EGF was quenched from 3.50 ns to 3.17 ns, corresponding to a distance of 7.9 nm, and the lifetime of Al-TGFα was quenched from 3.69 to 3.26 ns, corresponding to 7.7 nm. These results agreed to within 0.2 nm when the donor and acceptor labels on growth factor and Fab fragments were exchanged. This therefore points to the close proximity of the EGF and TGFα binding sites on the EGFR as measured from the extremity of the external domain. Whatever the origin of the apparent intergrowth factor distance difference for EGF and TGFα binding, however, the main conclusions of this work are unaffected.

In cells not pretreated with mAb 2E9, when a mixture of donor Al-TGFα and acceptor Er-TGFα was bound to EGFRs the donor lifetime was quenched to only 3.3 ns (bar 5), indicating the nonparticipation of low-affinity receptors in lifetime quenching and monomer-monomer separations in excess of that required for FRET. This was confirmed by the total absence of FRET observed when a 1:2 ratio of donor/acceptor TGFα was bound to A431R cells that have only low-affinity monomer EGFRs (bar 7 in Fig. 3 *A*).

High-affinity EGFRs are constitutive oligomers in A431 cells

To investigate the state of aggregation of high-affinity EGFRs before growth factor binding, A431 and A431R cells were reacted with a mixture of donor- and acceptor-conjugated Fab 29.1 fragments. EGFR oligomerization is distinguished by the quenching of the fluorescence lifetime of the donor antibody fragment conjugate. This antibody fragment, although not completely specific, as it is known to bind blood group-A carbohydrate antigens (Gooi et al., 1983), did not impede growth factor binding and therefore later enabled us to follow oligomerization after binding. The initial oligomeric state was also investigated using FRET measurements on donor- and acceptor-conjugated Fab fragments of the monoclonal anti-EGFR antibody 225, which exclusively binds to the EGF binding site and therefore prevents EGR binding (Gill et al., 1984). The donor fluorescence lifetimes of a 1:2 mixture of donor Al-Fab 29.1 and acceptor Er-Fab 29.1-bound A431 cells when compared with those from cells bound with a 1:2 mixture of Al-Fab 29.1 and unlabeled Fab 29.1, showed a decrease of 0.21 ns (bars 12 and 13 in Fig. 3 *A*). The quenching of the donor fluorescence lifetime with donor- and acceptor-conjugated Fab 225 bound to EGFRs in A431 cells by 0.19 ns confirmed that the Fab 29.1 fragment was indeed reporting the presence of oligomer EGFRs. No decrease in donor lifetime was detected in confluent A431R cells (bar 14 in Fig. 3 *A*), consistent with these cells being devoid of oligomers. These data provide evidence for a measurable population of high-affinity EGFR oligomers in A431 cells before growth factor binding, confirming recent results obtained in NIH3T3 cells (Moriki et al., 2001).

It could be argued that A431 cells, being a transformed cell line, could secrete sufficient TGFα (Derynck et al., 1987) to give a significant population of "apparent" constitutive oligomer receptors by growth factor-induced oligomerization. This oligomeric state could not then be termed constitutive. However, the FRET from donor- and acceptor-conjugated Fab 225 bound to A431 cells remained constant throughout a 5-min mild acid/salt extraction at 0°C (pH 4.5), a procedure known to dissociate the TGFα/EGFR complex (Ebner and Derynck, 1991). This leads us to the conclusion that autocrine binding of TGFα plays no significant part in forming the observed population of oligomers, which are therefore correctly termed constitutive because they are formed before growth factor binding.

Deriving distances from the fluorescence lifetime quenching of donor-conjugated Fabs in A431 cells proved more complex than for dye-conjugated growth factors bound to oligomeric EGFRs. In the latter case, blocking the binding of dye-conjugated growth factors to monomers rendered the lifetime analysis from oligomers trivial. This was not possible for dye-conjugated Fabs, whose fluorescence therefore contained two components from high-affinity EGFR oligomers and two components from non-energy-transferring monomers. The distance between Fab 29.1 molecules bound to oligomeric EGFRs was therefore computed using a multicomponent analysis of the fluorescence decay data. Although the two additional exponential values were determined from A431R cells and could therefore be entered as constant lifetimes in the analysis, the additional parameters to account for the pre-exponential components of the unquenched lifetimes resulted in a loss in precision. The analysis, however, returned a distance between Fab 29.1 fragments bound to high-affinity receptors in the range from 6 to 7 nm (Fig. 3 *B*). Fluorescence anisotropy values (Table 1) again showed a considerable freedom of rotation for the dye attached

to the Fab/EGFR complex discounting adverse orientation factors as a source of error in this calculation.

Using the fluorescence lifetime data given in Fig. 3 *A*, a projection scaffold model is shown in Fig. 3 *B* to summarize the FRET-derived average distances between ligands conjugated to high-affinity EGFR at 4°C. In this model we have made two assumptions: first, that all oligomeric EGFR are dimers; second, that these dimers have a twofold symmetry. The distances represent average distances between donor and acceptor fluorophores even though conjugates are labeled 1:1. We cannot claim that every fluorophore is covalently bound to unique sites.

A temperature-responsive structural change in EGFR's extracellular domain

FRET measurements were also used to investigate the changes in receptor oligomerization on binding unlabeled growth factor at 4°C and during the subsequent temperature jump to 37°C. The calculation of the time course for FRET efficiencies required two data sets from samples of cells grown under identical conditions. The first data set was recorded by collecting donor fluorescence decay profiles for a 1:2 ratio donor/acceptor bound species, an example of which is shown in Fig. 4 *A*. The second was from a similar procedure but with the acceptor-conjugated species replaced by unlabeled ligand (Fig. 4 *B*). In this way, the effect of changing the temperature on the fluorescence lifetime was removed from the calculation of FRET efficiencies.

The above method was used to monitor changes in the distance between EGFRs on addition of EGF. The time course for the efficiency of FRET for donor/acceptor-labeled Fab 29.1 bound to EGFRs on A431 cells is plotted in Fig. 5 *A*. The initial level of FRET arises from constitutive EGFR oligomers, albeit contaminated with a large fluorescence contribution from nontransferring donor EGFR monomers. When unlabeled EGF was added at 4°C there was no change in the FRET efficiency, and therefore major changes in distance between EGFR ectodomains did not occur at this temperature. A small, transient decrease in the efficiency of FRET between EGFR-bound Fab fragments was recorded for A431 cells on increasing the temperature from 4°C to 37°C (Fig. 5 *A*), but was not observed in A431R. This transient was not simply the response of the receptor's structure or the fluorophore emission to the temperature change because a similar transient was observed in donor/acceptor Fab-labeled A431 cells during exposure to a pulse of EGF at a constant 37°C (Fig. 5 *B*). The slower response to EGF at 4°C is presumably a result of stresses on the cells caused by refrigeration. As cells decorated with Fab 29.1 fragments underwent normal EGF-induced intracellular Ca^{2+} transients (Fig. 5 *C*) (Defize et al., 1989; Tinhofer et al., 1996; Peppelenbosch et al., 1996), we conclude that a transient distance increase between the extremities of the extracellular domains of high-affinity EGFR

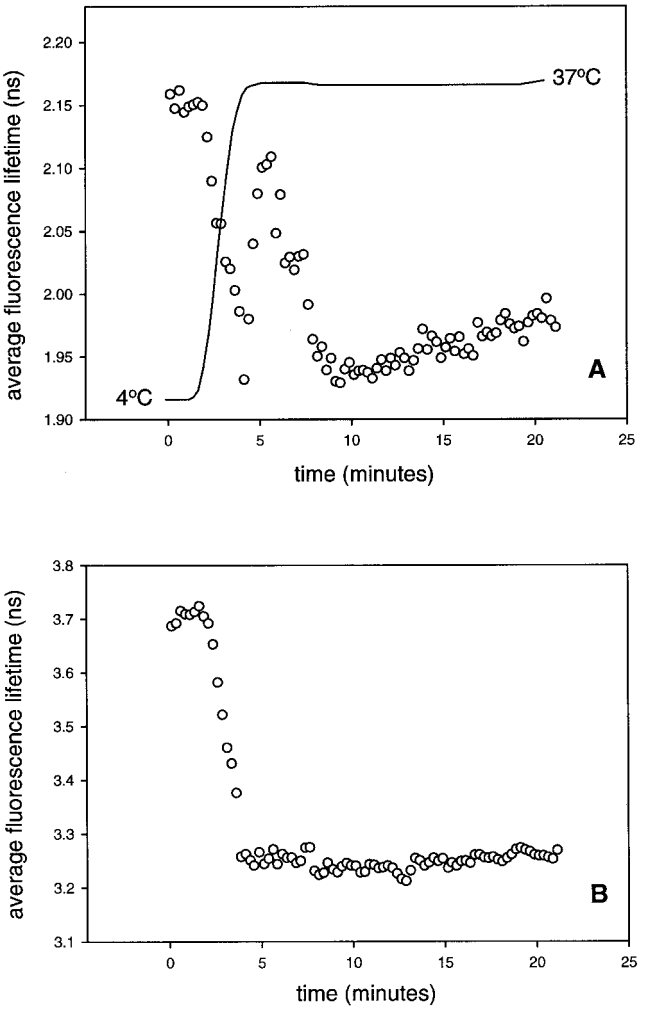

FIGURE 4 (*A*) Time course of the temperature change in cells (*continuous line*). Example of time course of the fluorescence lifetime of Al-TGFα bound to A431 cells at 4°C in a 1:2 ratio with acceptor Er-TGFα (uncorrected) after pretreatment with mAb 2E9 (*circles*). (*B*) Example of time course of the fluorescence lifetime of Al-TGFα in a 1:2 ratio with unlabeled TGFα. The fast initial decrease in (*A*) and (*B*) is a temperature-induced effect in the fluorescence lifetime.

occurs during EGFR signaling. This transient could be the result of a structural rearrangement within the external domains of oligomeric EGFR or the transitory dissociation and re-association of a proportion of oligomers.

The time course of the efficiency of FRET between donor/acceptor-labeled EGF molecules also showed a transient change on increasing the temperature from 4°C to 37°C (Fig. 6 *A*, *triangles*). This transient corresponds to a change in the distance between the fluorescent moieties of EGF molecules bound to high-affinity EGFR from 8.3 to 8.7 nm (Fig. 6 *B*, *triangles*). Cells exposed to antibody mAb 2E9 were also found to retain their signaling competence by a growth factor-induced transient increase in intracellular Ca^{2+} (Fig. 6 *B*, *continuous line*). A short time after the transient, the distance between EGF molecules began to increase progressively (Fig.

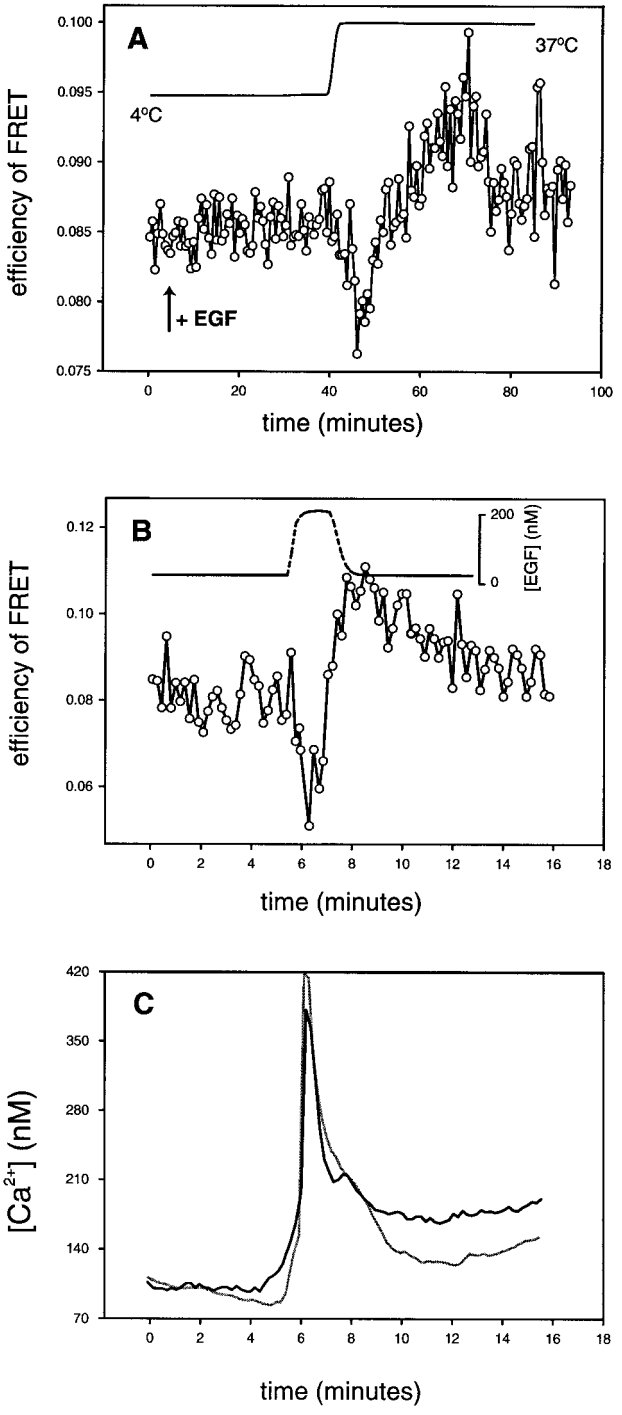

FIGURE 5 (*A*) Time course for the efficiency of FRET of Al-Fab 29.1 bound to A431 cells pretreated with Ca^{2+}-free buffer at 30 s per datum. An ice-cold solution of EGF (150 nM) was added at the time indicated by the arrow and rinsed with PBS before the temperature was increased to 37°C (*continuous line*). Results are the mean of at least three independent experiments with a variance of <10%. (*B*) As in (*A*), but at 11 s per datum. A 37°C solution of EGF (150 nM) in PBS was added to the cells and rinsed with PBS, as indicated by the figure (*dashed line*). (*C*) Time course of Ca^{2+} mobilization in A431 cells pre-equilibrated at 4°C with 300 nM unlabeled Fab 29.1, measured by monitoring Fluo-3 and Fura-Red fluorescence induced by the addition of a 150 nM solution of EGF (*black line*) or TGFα (*gray line*) in PBS, as shown in (*B*).

6 *B*, *triangles*), indicating either oligomer dissociation or the dissociation of EGF from oligomeric EGFRs. Fig. 6, *A* and *B* (*filled circles*), which report mostly on the majority monomer EGFR population, show a gradual increase in FRET over a period of 20 min after the temperature jump. This is indicative of a slow monomer secondary oligomerization phase, as previously shown (Gadella and Jovin, 1995; Blakely et al., 2000). However, the data in Fig. 6 *B* can only be interpreted qualitatively because of the large error introduced by the majority component of the fluorescence arising from nontransferring monomer EGFRs.

Changes in the efficiency of FRET between donor Al-EGF and acceptor Er-Fab 29.1 bound to dimer EGFRs in A431 cells were recorded and the corresponding distances calculated (Fig. 6, *A* and *B*, *open circles*). The distance between the fluorophores of Al-EGF and Er-Fab again shows a fast transient increase from 7.9 to 8.2 nm on raising the temperature from 4°C to 37°C. Unlike the time course of donor/acceptor-labeled EGF, the transient is not followed by the slow increase in inter-receptor distance. Therefore, this FRET occurs between dye-growth factor and dye-Fab 29.1 conjugates bound to the same EGFR ectodomain, and must reflect a structural change in the extracellular domain of EGFR. Moreover, this indicates that the slow increase in EGF-EGF separation after the FRET transient (Fig. 6, *A* and *B*, *open circles*) is due to EGFR oligomer dissociation rather than oligomer–growth factor dissociation.

The time course of FRET between donor Al-TGFα and acceptor Er-TGFα bound to high-affinity EGFRs after blocking low-affinity EGFRs with mAb 2E9 also showed a transient increase in the TGFα−TGFα distance from 5.7 to 5.9 nm in response to the temperature jump (Fig. 7, *A* and *B*, *triangles*). This transient was again followed by a slow progressive increase in distance as EGFR oligomers dissociate. The transient was much less pronounced when both high- and low-affinity EGFR were labeled, as for EGF, because of the high background from low-affinity monomer EGFRs (Fig. 7, *A* and *B*, *filled circles*). The distance between donor Al-TGFα and acceptor Er-Fab simultaneously bound to dimer EGFRs shows a similar transient increase to that for EGF signaling, from 7.7 to 7.9 nm (Fig. 7, *A* and *C*, *open circles*). No increase in the distance between TGFα and Fab 29.1 was observed after the transient, confirming that these distances report on the separation between a TGFα molecule and a Fab fragment bound to the same molecular component of the EGFR oligomer. These results confirm our previous conclusions from the EGF experiments.

DISCUSSION

The FRET data presented suggest that in A431 cells the binding of EGF or TGFα to high-affinity constitutive EGFR oligomers, i.e., the functional receptor moiety, leads to signal transduction and to a structural change in the receptor's extracellular domain. These results therefore indicate

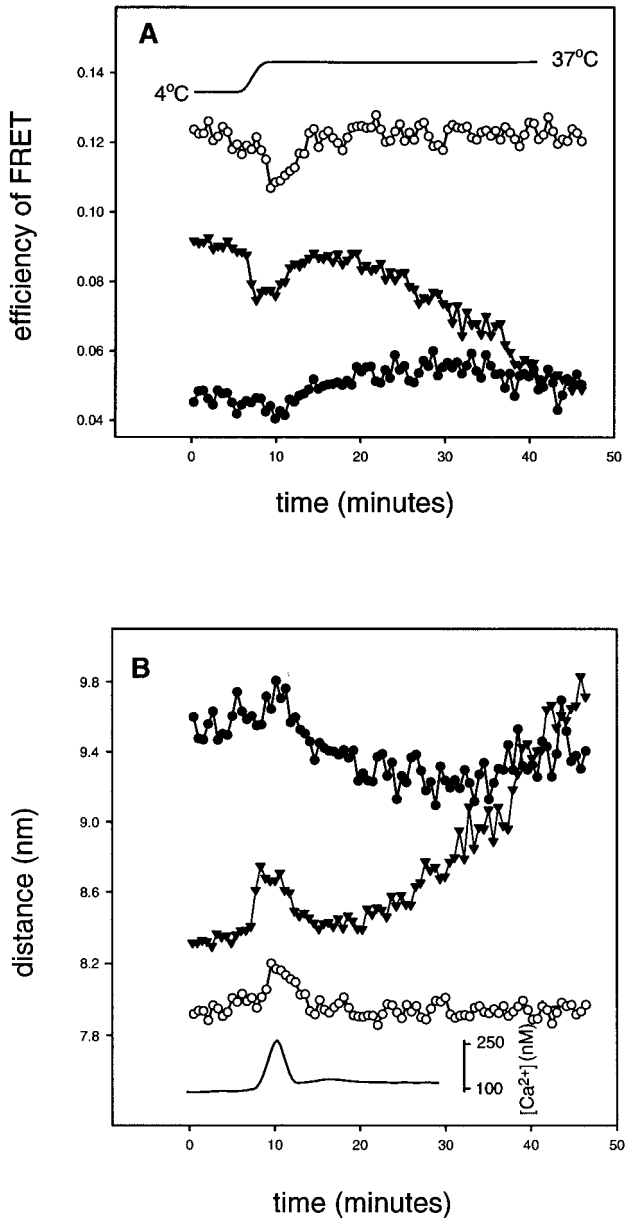

FIGURE 6 (*A*) Time course for the efficiency of FRET between donor/acceptor-labeled EGF bound to EGFRs during signaling as derived from fluorescence lifetime data following a temperature jump from 4°C to 37°C (*continuous line*). Efficiency of transfer between Al-EGF and Er-EGF bound to surface EGFRs in A431 cells pretreated with Ca^{2+}-free buffer (*filled circles*); Al-EGF and Er-Fab (*open circles*); and high-affinity Al-EGF and Er-EGF in cells pretreated with mAb 2E9 (*triangles*). (*B*) Time course for the distance between Al-EGF and Er-EGF bound to both high- and low-affinity EGFRs (*filled circles*); Al-EGF and Er-EGF bound to high-affinity EGFRs (*triangles*); and Al-EGF and Er-Fab (*open circles*) calculated from the FRET efficiency data. Results are the mean of at least three independent experiments with a variance of <5%. EGF-induced Ca^{2+} mobilization originated by high-affinity EGFR binding followed by monitoring Fluo-3 and Fura-Red fluorescence (*continuous line*).

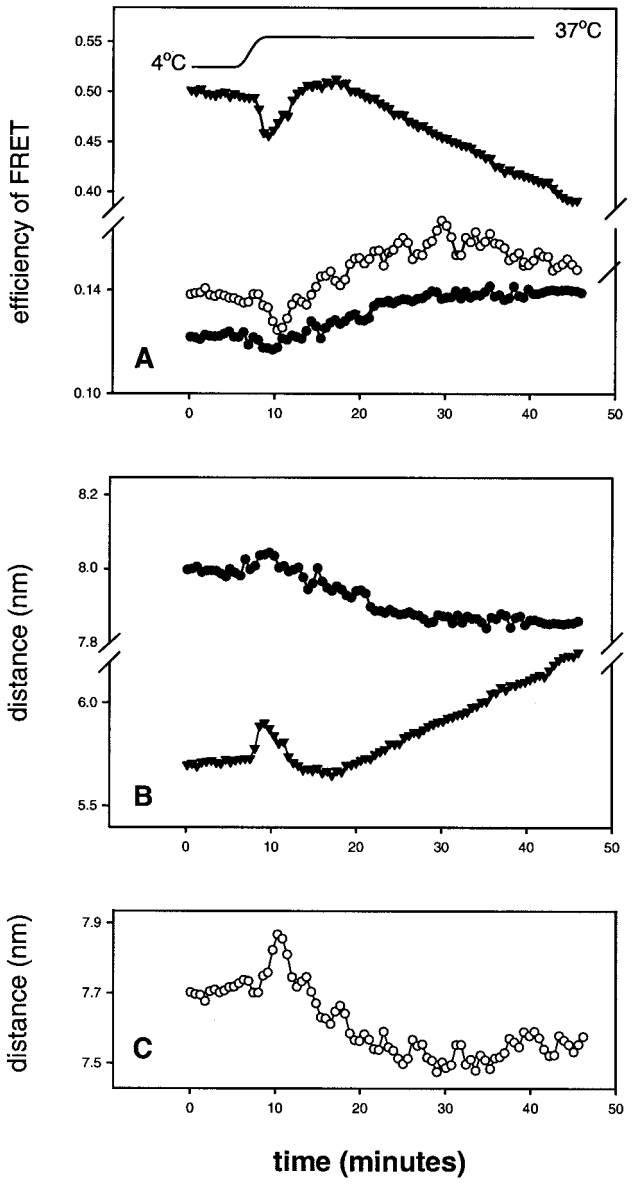

FIGURE 7 (*A*) Time course for the efficiency of FRET between donor/acceptor-labeled TGFα bound to EGFRs during signaling as derived from fluorescence lifetime data following a temperature jump from 4°C to 37°C (*continuous line*). Efficiency of transfer between Al-TGFα and Er-TGFα bound to surface EGFRs in A431 cells pretreated with Ca^{2+}-free buffer (*filled circles*); Al-TGFα and Er-Fab (*open circles*); and high-affinity Al-TGFα and Er-TGFα in cells that had been pretreated with mAb 2E9 (*triangles*). (*B*) Time course of the distance between Al-TGFα and Er-TGFα bound to both high- and low-affinity surface EGFRs (*filled circles*), and high-affinity EGFRs (*triangles*), calculated from the FRET efficiency data. (*C*) Distance between Al-TGFα and Er-Fab (*open circles*). Results are the mean of at least three independent experiments with a variance of <5%.

that ligand-induced oligomerization cannot be an absolute requirement for the onset of RTK signal transduction, as suggested by the allosteric signaling mechanism of RTK activation (Schlessinger, 1988).

The existence of constitutive oligomer EGFRs (probably dimers) (Sako et al., 2000), has previously been reported. A

small level of pre-dimerization has been found in live A431 cells by cross-linking and β-galactosidase complementation studies (Böni-Schnetzler and Pilch, 1987; Cochet et al., 1988; Sorokin et al., 1994; Chu et al., 1997; Blakely et al., 2000). Preformed EGF receptor dimers have also been found in NIH3T3 cells using chemical cross-linking and sucrose density-gradient centrifugation (Moriki et al., 2001). For other receptors, x-ray crystallography, spectroscopic, and biochemical methods have also demonstrated the existence of inactive pre-dimerized erythropoietin receptors (EPOR), tumor necrosis factor, and Neu receptors (review by Jiang and Hunter, 1999). However, in the case of A431 cells it could be argued that the presence of constitutive oligomeric EGFRs might merely be a product of EGFR overexpression. We do not think this can be the case for two reasons: first, because A431R cells, which overexpress EGFR to identical levels (Nelson and Fry, 1997), have far less constitutive oligomers (Fig. 3); second, because chemical cross-linking and sucrose density-gradient centrifugation data have shown that in NIH3T3 cells, which express EGFR at physiological levels, EGFR forms constitutive dimers at the cell surface (Moriki et al., 2001). There is sufficient evidence for the presence of constitutive oligomers for their role in signal transduction to have some significance.

The binding of EGF to EGFRs is known to promote RTK activation even at 4°C (McCune and Earp, 1989; Sorokin et al., 1994; Ringerike et al., 1998). At 4°C, however, our FRET results (Fig. 5 *A*) suggest that EGF binding does not cause structural changes that result in a significant increase in distance between EGFR ectodomains, which would be measurable by FRET. The absence of FRET changes therefore suggests that tyrosine kinase activity in EGFR is not associated with the "rocking motion"-like structural changes observed in EPOR, which have been shown to lead to receptor activation (Remy et al., 1999). Our data are, however, consistent with the "flexible rotation" model for EGFR activation proposed by Moriki et al. (2001), as the reported EGF-induced rotation of the transmembrane domain would not result in significant distance changes between EGFR ectodomains. In contrast with our FRET results at 4°C, the growth factor-induced structural change observed on raising the temperature to 37°C (Figs. 4, 6, and 7), which must therefore occur after EGFR tyrosine kinase activation, is consistent with a rocking motion similar to that described for EPOR (Remy et al., 1999). If this structural change has any physiological relevance, it might be related to one or several of the temperature-responsive processes occurring in EGFR signaling. Examples of these processes are EGFR's phosphorylation of substrates (McCune and Earp, 1989); formation of ruffles (Rijken et al., 1991); high-affinity EGFR binding to actin microfilaments (Zidovetzki et al., 1991); desensitization of EGFR, by which EGFR loses the ability to dimerize in response to a second EGF challenge (Kuppuswamy and Pike, 1989); and the production of Ca^{2+} second messenger (Fig. 6 *B*). Ca^{2+} transients have been shown to be mediated by EGFR's phosphorylation of the oncogenic GTP-binding proteins Ras and Rac (Tinhofer et al., 1996; Peppelenbosch et al., 1996), the latter directly mediating the formation of ruffles (Ridley et al., 1992). The excellent time correlation between the structural change in EGFR and the measured Ca^{2+} transients (Figs. 5 and 6) suggests that these two events might be related. It is therefore possible that the transient structural change in the extracellular domain of EGFRs can be one of the events facilitating the binding of EGFR cytoplasm domain to those substrates generating growth factor-induced Ca^{2+} transients.

In summary, the work described here provides for some insight on the mechanisms of EGFR signal transduction. In agreement with previous reports (Gadella and Jovin, 1995; Verveer et al., 2000; Moriki et al., 2001), our data have shown that ligand-induced EGFR dimerization is not the only mechanism of EGFR activation, and have found evidence for a new signaling role for constitutive oligomeric EGFRs. We have also provided data in support of the occurrence of a structural change in the ectodomain of EGFR, which may be necessary for signals to occur. The observed rapid dissociation of EGFR after undergoing the transient structure change suggests that EGFR dimers are not stable for very long after signaling. It is conceivable that the newly dissociated receptors could subsequently interact with unliganded nonphosphorylated monomeric EGFRs to form secondary oligomers, and in this way propagate signals along the plasma membrane, as previously observed by other methods (Defize et al., 1989; Gamett et al., 1997; Verveer et al., 2000).

We thank J. Oliver, C. Bithell, and D. Walker for their invaluable assistance throughout this work.

We also thank the BBSRC for funding SRS beam time and Grants 637/SYS4704 and 719/C09632.

REFERENCES

Aboud-Pirak, E., E. Hurwitz, M. E. Pirak, F. Bellot, J. Schlessinger, and M. Sela. 1988. Efficiency of antibodies to epidermal growth factor receptor against KB carcinoma in vitro and in nude mice. *J. Natl. Cancer Inst.* 80:1605–1611.

Bellot, F., W. Moolenaar, R. Kris, B. Mirakhur, I. Verlaan, A. Ullrich, J. Schlessinger, and S. Felder. 1990. High-affinity epidermal growth factor binding is specifically reduced by a monoclonal antibody, and appears necessary for early responses. *J. Cell Biol.* 100:491–502.

Blakely, B. T., F. M. V. Rossi, B. Tillotson, M. Palmer, A. Estelles, and H. M. Blau. 2000. Epidermal growth factor receptor dimerization monitored in live cells. *Nature Biotech.* 18:218–222.

Böni-Schnetzler, M., and P. F. Pilch. 1987. Mechanism of epidermal growth factor receptor autophosphorylation and high-affinity binding. *Proc. Natl. Acad. Sci. U.S.A.* 84:7832–7836.

Boonstra, J., C. L. Mummery, P. T. Van der Saag, and S. W. De Laat. 1985. Receptor classes for epidermal growth-factor on pheochromocytoma cells, distinguishable by temperature, lectins, and tumor promoters. *J. Cell Physiol.* 123:347–352.

Brown, M. S., and J. L. Goldstein. 1979. Receptor-mediated endocytosis: insights from the lipoprotein receptor system. *Proc. Natl. Acad. Sci. U.S.A.* 76:3330–3337.

Carpenter, G. 1987. Receptors for epidermal growth factors and other polypeptide mitogens. *Annu. Rev. Biochem.* 56:881–914.

Carpenter, G. 2000. The EGF receptor: a nexus for trafficking and signaling. *BioEssays.* 22:697–707.

Carpenter, G., and S. Cohen. 1979. Epidermal growth factor. *Annu. Rev. Biochem.* 48:193–216.

Chantry, A. 1995. The kinase domain and membrane localization determine intracellular interactions between epidermal growth-factor receptors. *J. Biol. Chem.* 270:3068–3073.

Chu, C. T., K. D. Everiss, C. J. Wikstrand, S. K. Batra, H. Jung, and D. D. Bigner. 1997. Receptor dimerization is not a factor in the signaling activity of a transforming variant epidermal growth factor receptor (EGFRvIII). *Biochem. J.* 324:855–861.

Cochet, C., O. Kashles, E. M. Chambaz, I. Borrello, C. R. King, and J. Schlessinger. 1988. Demonstration of epidermal growth factor-induced receptor dimerization in living cells using a chemical covalent cross-linking agent. *J. Biol. Chem.* 263:3290–3295.

Defize, L. H. K., J. Boonstra, J. Meisenhelder, W. Kruijer, L. G. J. Tertoolen, B. C. Tilli, T. Hunter, P. M. P. van Bergen en Henegouwen, W. H. Moolenar, and S. W. de Laat. 1989. Signal transduction by epidermal growth factor occurs through the subclass of high-affinity receptors. *J. Cell Biol.* 109:2495–2507.

Derynck, R. D. V. Goeddel, A. Ullrich, J. U. Gutterman, R. D. Williams, T. S. Bringman, and W. Berger. 1987. Synthesis of messenger RNAs for transforming growth factors a and b and the epidermal growth factor receptor by human tumors. *Cancer Res.* 47:707–712.

Derynck, R., A. B. Roberts, M. E. Winkler, E. Y. Chewn, and D. V. Goedel. 1984. Human transforming growth factor-alpha: precursor structure and expression in *E. coli*. *Cell.* 38:287–297.

Ebner, E., and R. Derynck. 1991. Epidermal growth factor and transforming growth factor-a: differential intracellular routing and processing of ligand-receptor complexes. *Cell Regul.* 2:599–612.

Fabricant, R. N., J. E. De Larco, and G. J. Todaro. 1977. Nerve growth factor receptors on human melanoma cells. *Proc. Natl. Acad. Sci. U.S.A.* 74:565–569.

Gadella, Jr., T. W. J., and T. M. Jovin. 1995. Oligomerization of epidermal growth factor receptors on A431 cells studied by time-resolved fluorescence imaging microscopy: a stereochemical model for tyrosine kinase receptor activation. *J. Cell Biol.* 129:1543–1558.

Gamett, D. C., G. Pearson, R. A. Cerione, and I. Friedberg. 1997. Secondary dimerization between members of the growth factor receptor family. *J. Biol. Chem.* 272:12052–12056.

Gill, G. N., T. Kawamoto, C. Cochet, A. Le, J. D. Sato, H. Masui, C. McLeod, and J. Mendelsohn. 1984. Monoclonal anti-epidermal growth-factor receptor antibodies which are inhibitors of epidermal growth-factor binding and antagonists of epidermal growth factor stimulated tyrosine protein-kinase activity. *J. Biol. Chem.* 259:7755–7760.

Gooi, H. C., J. Schlessinger, I. Lax, Y. Yarden, T. A. Libermann, and T. Feizi. 1983. Monoclonal antibody reactive with the human epidermal growth factor receptor recognizes the blood-group-A antigen. *Biosci. Rep.* 3:1045–1052.

Gregory, C. M., M. A. Hayes, E. Pantos, and G. R. Jones. 1994. FLUOR: a program to analyse fluorescence data. *Daresbury Laboratory Technical Memorandum* DL/SCI/TM98E.

Haas, E., E. Katchalski-Katzir, and I. Z. Steinberg. 1978. Effect of the orientation of donor and acceptor on the probability of energy transfer involving electronic transitions of mixed polarization. *Biochemistry.* 17:5064–5070.

Hartmann, P., M. J. P. Leiner, and P. Kohlbacher. 1998. Photobleaching of a ruthenium complex in polymers used for oxygen optodes and its inhibition by singlet oxygen quenchers. *Sensor Actuat. B-Chem.* 51: 196–202.

Harvey, T. S., A. J. Wilkinson, M. J. Tappin, R. M. Cooke, and I. D. Campbell. 1991. The solution structure of human transforming growth factor alpha. *Eur. J. Biochem.* 198:555–562.

Holley, R. W., R. Armour, J. H. Baldwin, K. D. Brown, and Y.-C. Yeh. 1977. Density-dependent regulation control of growth of BSC-1 cells in cell culture: control of growth by serum factors. *Proc. Natl. Acad. Sci. U.S.A.* 74:5046–5050.

Hubbard, S. R., L. Wei, L. Ellis, and W. A. Hendrickson. 1994. Crystal structure of the tyrosine kinase domain of the human insulin receptor. *Nature.* 372:746–754.

Hunter, T., and J. A. Cooper. 1981. Epidermal growth factor induces rapid tyrosine phosphorylation of proteins in A431 human tumor cells. *Cell.* 24:741–752.

Jiang, G., and T. Hunter. 1999. Receptor signaling: when dimerization is not enough. *Curr. Biol.* 9:568–571.

Kohda, D., and F. Inagaki. 1992. Three-dimensional nuclear magnetic resonance structures of mouse epidermal growth factor in acidic and physiological pH solutions. *Biochemistry.* 31:11928–11939.

Kuppuswamy, D., and L. J. Pike. 1989. Ligand-induced desensitization of ^{125}I-epidermal growth factor internalization. *J. Biol. Chem.* 264: 3357–3363.

Lakowicz, J. R. 1983. Principles of Fluorescence Spectroscopy. Plenum, New York.

Lemmon, M. A., Z. Bu, J. E. Ladbury, M. Zhou, D. Pinchasi, I. Lax, D. M. Engelman, and J. Schlessinger. 1997. Two EGF molecules contribute additively to stabilization of the EGFR dimer. *EMBO J.* 16:281–294.

Lichtner, R. B., and V. Schirrmacher. 1990. Cellular distribution and biological activity of epidermal growth factor receptors in A431 cells are influenced by cell-cell contact. *J. Cell. Physiol.* 144:303–312.

Martin-Fernandez, M. L., M. J. Tobin, D. T. Clarke, C. M. Gregory, and G. R. Jones. 1996. A high sensitivity time-resolved microfluorimeter for real-time cell biology. *Rev. Sci. Instrum.* 67:3716–3721.

Martin-Fernandez, M. L., M. J. Tobin, D. T. Clarke, C. M. Gregory, and G. R. Jones. 1998. Sub-nanosecond polarized microfluorimetry in the time domain: an instrument for studying receptor trafficking in live cells. *Rev. Sci. Instrum.* 69:540–543.

McCune, B. K., and H. S. Earp. 1989. The epidermal growth factor receptor tyrosine kinase in liver epithelial cells. *J. Biol. Chem.* 264: 15501–15507.

Moriki, T., H. Maruyama, and I. N. Maruyama. 2001. Activation of preformed EGF receptor dimers by ligand-induced rotation of the transmembrane domain. *J. Mol. Biol.* 311:1011–1026.

Nelson, J. M., and D. Fry. 1997. Cytoskeletal and morphological changes associated with the specific suppression of the epidermal growth factor receptor tyrosine kinase activity in A431 human epidermoid carcinoma. *Exp. Cell Res.* 233:383–390.

Novak, E. J., and P. S. Rabinovitch. 1994. Improved sensitivity in flow cytometric intracellular ionized calcium measurement using fluo-3 fura red fluorescence ratios. *Cytometry.* 17:135–141.

Pawson, T. 1995. Protein modules and signaling networks. *Nature.* 373: 573–580.

Peppelenbosch, M. P., L. G. J. Tertoolen, A. M. M. de Vries-Smits, R.-G. Qiu, L. M'Rabet, M. H. Symons, S. W. de Laat, and J. L. Bos. 1996. Rac-dependent and -independent pathways mediate growth factor-induced Ca^{2+} influx. *J. Biol. Chem.* 271:7883–7886.

Plotnikov, A. N., J. Schlessinger, S. R. Hubbard, and M. Mohammadi. 1999. Structural basis for FGF receptor dimerization and activation. *Cell.* 98:641–650.

Rees, A. R., M. Gregoriou, P. Johson, and P. B. Garland. 1984. High-affinity epidermal growth factor receptors on the surface of A431 cells have restricted lateral diffusion. *EMBO J.* 3:1843–1847.

Remy, I., I. A. Wilson, and S. W. Michnick. 1999. Erythropoietin receptor activation by a ligand-induced conformational change. *Science.* 283: 990–993.

Ridley, A. J., H. F. Paterson, C. L. Johnston, D. Diekmann, and A. Hall. 1992. The small GTP-binding protein Rac regulates growth factor-induced membrane ruffling. *Cell.* 70:404–410.

Rijken, P. J., W. J. Hage, P. M. P. van Bergen en Henegouwen, A. J. Verkleij, and J. Boonstra. 1991. Epidermal growth factor induces rapid reorganization of the actin microfilament in human A431 cells. *J. Cell Sci.* 100:491–499.

Ringerike, T., E. Stang, L. E. Johannessen, D. Sandness, F. Olav Levy, and I. H. Madshus. 1998. High-affinity binding of epidermal growth factor (EGF) to EGF receptor is disrupted by overexpression of mutant dynamin (K44A). *J. Biol. Chem.* 273:16639–16642.

Sako, Y., S. Minoghchi, and T. Yanagida. 2000. Single-molecule imaging of EGFR signaling on the surface of living cells. *Nature Cell Biol.* 2:168–173.

Schlessinger, J. 1988. Signal transduction by allosteric receptor oligomerization. *Trends Biochem. Sci.* 13:443–447.

Schreiber, A. B., T. A. Libermann, I. Lax, Y. Yarden, and J. Schlessinger. 1983. Biological role of epidermal growth factor-receptor clustering. *J. Biol. Chem.* 258:846–853.

Sorokin, A., M. A. Lemmon, and J. Schlessinger. 1994. Stabilization of an active dimeric form of the epidermal growth factor receptor by introduction of an inter-receptor disulfide bond. *J. Biol. Chem.* 269: 9752–9759.

Stryer, L., and R. P. Haugland. 1967. Energy transfer: a spectroscopic ruler. *Proc. Natl. Acad. Sci. U.S.A.* 58:719–726.

Suarez-Quian, C. A., and S. W. Byers. 1993. Redistribution of epidermal growth factor receptor as a function of cell density, cell-cell adhesion, and calcium in human A431 cells. *Tissue Cell.* 25:1–17.

Tinhofer, I., K. Maly, P. Dietl, F. Hochholdinger, S. Mayr, A. Obermeier, and H. H. Grunicke. 1996. Differential Ca^{2+} signaling induced by activation of the epidermal growth factor and nerve growth factor receptors. *J. Biol. Chem.* 39:30505–30509.

Verveer, P. J., F. S. Wouters, A. R. Reynolds, and P. I. H. Bastiaens. 2000. Quantitative imaging of lateral ErbB1 receptor signal propagation in the plasma membrane. *Science.* 290:1567–1570.

Winkler, M. E., L. O'Connor, M. Winget, and B. Fendly. 1989. Epidermal growth factor and transforming growth factor a bind differently to the epidermal growth factor receptor. *Biochemistry.* 28:6373–6378.

Yarden, Y., I. Harari, and J. Schlessinger. 1985. Purification of an active EGF receptor kinase with monoclonal antireceptor antibodies. *J. Biol. Chem.* 260:315–319.

Yarden, Y., and J. Schlessinger. 1987a. Self-phosphorylation of epidermal growth factor: evidence for a model of intermolecular allosteric activation. *Biochemistry.* 26:1434–1442.

Yarden, Y., and J. Schlessinger. 1987b. Epidermal growth factor induces rapid, reversible aggregation of the purified epidermal growth factor receptor. *Biochemistry.* 26:1443–1451.

Zidovetzki, R., D. A. Johnson, D. J. Arndt-Jovin, and T. M. Jovin. 1991. Rotational mobility of high-affinity epidermal growth factor receptors in the surface of living A431 cells. *Biochemistry.* 30:6162–6166.